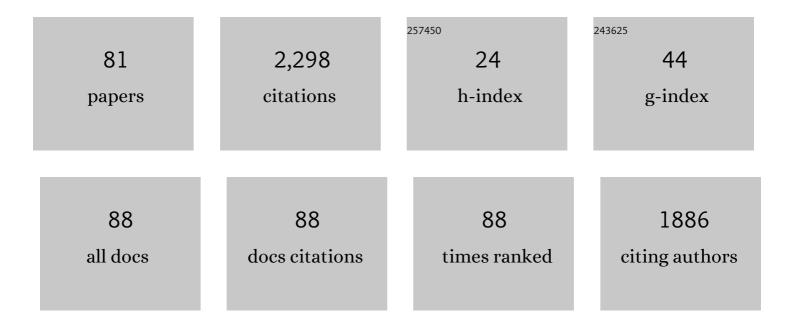
List of Publications by Year in descending order

Source: https://exaly.com/author-pdf/7743973/publications.pdf Version: 2024-02-01



#	Article	IF	CITATIONS
1	Longitudinal1H Relaxation Optimization in TROSY NMR Spectroscopy. Journal of the American Chemical Society, 2002, 124, 12898-12902.	13.7	166
2	An enzymatic molten globule: Efficient coupling of folding and catalysis. Proceedings of the National Academy of Sciences of the United States of America, 2004, 101, 12860-12864.	7.1	128
3	Limits on Variations in Protein Backbone Dynamics from Precise Measurements of Scalar Couplings. Journal of the American Chemical Society, 2007, 129, 9377-9385.	13.7	127
4	The nuclear Overhauser effect from a quantitative perspective. Progress in Nuclear Magnetic Resonance Spectroscopy, 2014, 78, 1-46.	7.5	115
5	Structure and dynamics of a molten globular enzyme. Nature Structural and Molecular Biology, 2007, 14, 1202-1206.	8.2	102
6	NMR Determination of Amide Nâ^'H Equilibrium Bond Length from Concerted Dipolar Coupling Measurements. Journal of the American Chemical Society, 2008, 130, 16518-16520.	13.7	98
7	Targeting tumor-derived NLRP3 reduces melanoma progression by limiting MDSCs expansion. Proceedings of the National Academy of Sciences of the United States of America, 2021, 118, .	7.1	95
8	Spatial elucidation of motion in proteins by ensemble-based structure calculation using exact NOEs. Nature Structural and Molecular Biology, 2012, 19, 1053-1057.	8.2	92
9	Exact Distances and Internal Dynamics of Perdeuterated Ubiquitin from NOE Buildups. Journal of the American Chemical Society, 2009, 131, 17215-17225.	13.7	91
10	Simultaneous NMR Study of Protein Structure and Dynamics Using Conservative Mutagenesis. Journal of Physical Chemistry B, 2008, 112, 6045-6056.	2.6	87
11	Relaxation Matrix Analysis of Spin Diffusion for the NMR Structure Calculation with eNOEs. Journal of Chemical Theory and Computation, 2012, 8, 3483-3492.	5.3	47
12	Solution NMR Studies of Recombinant Aβ(1–42): From the Presence of a Micellar Entity to Residual βâ€5heet Structure in the Soluble Species. ChemBioChem, 2015, 16, 659-669.	2.6	42
13	Correlated Dynamics between Protein HN and HC Bonds Observed by NMR Cross Relaxation. Journal of the American Chemical Society, 2009, 131, 3668-3678.	13.7	39
14	The Exact NOE as an Alternative in Ensemble Structure Determination. Biophysical Journal, 2016, 110, 113-126.	0.5	39
15	A transient helix in the disordered region of dynein light intermediate chain links the motor to structurally diverse adaptors for cargo transport. PLoS Biology, 2019, 17, e3000100.	5.6	39
16	Recognition of non-CpG repeats in Alu and ribosomal RNAs by the Z-RNA binding domain of ADAR1 induces A-Z junctions. Nature Communications, 2021, 12, 793.	12.8	39
17	Structure and dynamics conspire in the evolution of affinity between intrinsically disordered proteins. Science Advances, 2018, 4, eaau4130.	10.3	38
18	Detection of C′,Cα correlations in proteins using a new time- and sensitivity-optimal experiment. Journal of Biomolecular NMR, 2005, 31, 273-278.	2.8	33

#	Article	IF	CITATIONS
19	Quantitative determination of NOE rates in perdeuterated and protonated proteins: Practical and theoretical aspects. Journal of Magnetic Resonance, 2010, 204, 290-302.	2.1	32
20	eNORA2 Exact NOE Analysis Program. Journal of Chemical Theory and Computation, 2017, 13, 4336-4346.	5.3	32
21	Towards a true protein movie: A perspective on the potential impact of the ensemble-based structure determination using exact NOEs. Journal of Magnetic Resonance, 2014, 241, 53-59.	2.1	31
22	Integrating NMR and simulations reveals motions in the UUCG tetraloop. Nucleic Acids Research, 2020, 48, 5839-5848.	14.5	31
23	A Structural Ensemble for the Enzyme Cyclophilin Reveals an Orchestrated Mode of Action at Atomic Resolution. Angewandte Chemie - International Edition, 2015, 54, 11657-11661.	13.8	30
24	Microbiota-derived butyrate is an endogenous HIF prolyl hydroxylase inhibitor. Gut Microbes, 2021, 13, 1938380.	9.8	30
25	The Inherent Dynamics and Interaction Sites of the SARS-CoV-2 Nucleocapsid N-Terminal Region. Journal of Molecular Biology, 2021, 433, 167108.	4.2	30
26	Multiple-state ensemble structure determination from eNOE spectroscopy. Molecular Physics, 2013, 111, 437-454.	1.7	28
27	Protein backbone motions viewed by intraresidue and sequential HN–Hα residual dipolar couplings. Journal of Biomolecular NMR, 2008, 41, 17-28.	2.8	27
28	The Exact Nuclear Overhauser Enhancement: Recent Advances. Molecules, 2017, 22, 1176.	3.8	26
29	Simultaneous 1H- or 2H-, 15N- and multiple-band-selective 13C-decoupling during acquisition in 13C-detected experiments with proteins and oligonucleotides. Journal of Biomolecular NMR, 2005, 31, 1-9.	2.8	24
30	Measurements of Side-Chain13Câ~'13C Residual Dipolar Couplings in Uniformly Deuterated Proteins. Journal of the American Chemical Society, 2004, 126, 2414-2420.	13.7	23
31	The Structure of Mouse Cytomegalovirus m04 Protein Obtained from Sparse NMR Data Reveals a Conserved Fold of the m02-m06 Viral Immune Modulator Family. Structure, 2014, 22, 1263-1273.	3.3	23
32	Extending the eNOE data set of large proteins by evaluation of NOEs with unresolved diagonals. Journal of Biomolecular NMR, 2015, 62, 63-69.	2.8	23
33	High-resolution small RNA structures from exact nuclear Overhauser enhancement measurements without additional restraints. Communications Biology, 2018, 1, 61.	4.4	23
34	Spin-State Selective Carbon-Detected HNCO with TROSY Optimization in All Dimensions and Double Echoâ^'Antiecho Sensitivity Enhancement in Both Indirect Dimensions. Journal of the American Chemical Society, 2007, 129, 5484-5491.	13.7	21
35	Protein Allostery at Atomic Resolution. Angewandte Chemie - International Edition, 2020, 59, 22132-22139.	13.8	21
36	Deuteration of nonexchangeable protons on proteins affects their thermal stability, side•hain dynamics, and hydrophobicity. Protein Science, 2020, 29, 1641-1654.	7.6	21

#	Article	IF	CITATIONS
37	Comprehensive description of NMR cross-correlated relaxation under anisotropic molecular tumbling and correlated local dynamics on all time scales. Journal of Chemical Physics, 2010, 133, 014501.	3.0	20
38	The Dynamic Basis for Signal Propagation in Human Pin1-WW. Structure, 2016, 24, 1464-1475.	3.3	20
39	Exact distance measurements for structure and dynamics in solid proteins by fast-magic-angle-spinning NMR. Chemical Communications, 2019, 55, 7899-7902.	4.1	20
40	Complementarity and congruence between exact NOEs and traditional NMR probes for spatial decoding of protein dynamics. Journal of Structural Biology, 2015, 191, 306-317.	2.8	19
41	Direct Investigation of Slow Correlated Dynamics in Proteins via Dipolar Interactions. Journal of the American Chemical Society, 2016, 138, 8412-8421.	13.7	19
42	The experimental accuracy of the uni-directional exact NOE. Journal of Magnetic Resonance, 2015, 259, 32-46.	2.1	17
43	Microbialâ€derived indoles inhibit neutrophil myeloperoxidase to diminish bystander tissue damage. FASEB Journal, 2021, 35, e21552.	0.5	17
44	Temperature Dependence of1HN–1HNDistances in Ubiquitin As Studied by Exact Measurements of NOEs. Journal of Physical Chemistry B, 2011, 115, 7648-7660.	2.6	16
45	Stereospecific assignments in proteins using exact NOEs. Journal of Biomolecular NMR, 2013, 57, 211-218.	2.8	16
46	Extending the Applicability of Exact Nuclear Overhauser Enhancements to Large Proteins and RNA. ChemBioChem, 2018, 19, 1695-1701.	2.6	15
47	TROSY experiment for refinement of backbone psi and phi by simultaneous measurements of cross-correlated relaxation rates and 3,4J(H alpha HN) coupling constants. Journal of Biomolecular NMR, 2002, 24, 291-300.	2.8	13
48	Enzyme Selectivity Fineâ€Tuned through Dynamic Control of a Loop. Angewandte Chemie - International Edition, 2016, 55, 3096-3100.	13.8	13
49	Reconstruction of Coupled Intra- and Interdomain Protein Motion from Nuclear and Electron Magnetic Resonance. Journal of the American Chemical Society, 2021, 143, 16055-16067.	13.7	13
50	Compiled data set of exact NOE distance limits, residual dipolar couplings and scalar couplings for the protein GB3. Data in Brief, 2015, 5, 99-106.	1.0	11
51	Protein Motional Details Revealed by Complementary Structural Biology Techniques. Structure, 2020, 28, 1024-1034.e3.	3.3	11
52	The Disordered Spindly C-terminus Interacts with RZZ Subunits ROD-1 and ZWL-1 in the Kinetochore through the Same Sites in C. Elegans. Journal of Molecular Biology, 2021, 433, 166812.	4.2	11
53	Observation of Individual Transitions in Magnetically Equivalent Spin Systems. Journal of the American Chemical Society, 2003, 125, 9566-9567.	13.7	10
54	Discrete Three-dimensional Representation of Macromolecular Motion from eNOE-based Ensemble Calculation. Chimia, 2012, 66, 787.	0.6	10

#	Article	IF	CITATIONS
55	Side-chain H and C resonance assignment in protonated/partially deuterated proteins using an improved 3D13C-detected HCC–TOCSY. Journal of Magnetic Resonance, 2005, 174, 200-208.	2.1	9
56	Side chain: backbone projections in aromatic and ASX residues from NMR cross-correlated relaxation. Journal of Biomolecular NMR, 2010, 46, 135-147.	2.8	9
57	Cross-correlated relaxation rates between protein backbone H–X dipolar interactions. Journal of Biomolecular NMR, 2017, 67, 211-232.	2.8	9
58	NOEâ€Đerived Methyl Distances from a 360 kDa Proteasome Complex. Chemistry - A European Journal, 2018, 24, 2270-2276.	3.3	9
59	How uniform is the peptide plane geometry? A high-accuracy NMR study of dipolar Cα–C′/HN–N cross-correlated relaxation. Journal of Biomolecular NMR, 2011, 50, 315-329.	2.8	8
60	Distanceâ€independent Crossâ€correlated Relaxation and Isotropic Chemical Shift Modulation in Protein Dynamics Studies. ChemPhysChem, 2019, 20, 178-196.	2.1	8
61	Efficient Stereospecific Hβ2/3 NMR Assignment Strategy for Mid-Size Proteins. Magnetochemistry, 2018, 4, 25.	2.4	7
62	Reducing the measurement time of exact NOEs by non-uniform sampling. Journal of Biomolecular NMR, 2020, 74, 717-739.	2.8	7
63	Activity and Affinity of Pin1 Variants. Molecules, 2020, 25, 36.	3.8	7
64	The Sign of Nuclear Magnetic Resonance Chemical Shift Difference as a Determinant of the Origin of Binding Selectivity: Elucidation of the Position Dependence of Phosphorylation in Ligands Binding to Scribble PDZ1. Biochemistry, 2018, 57, 66-71.	2.5	6
65	Backbone and side-chain chemical shift assignments of full-length, apo, human Pin1, a phosphoprotein regulator with interdomain allostery. Biomolecular NMR Assignments, 2019, 13, 85-89.	0.8	6
66	Intermolecular Detergent–Membrane Protein NOEs for the Characterization of the Dynamics of Membrane Protein–Detergent Complexes. Journal of Physical Chemistry B, 2014, 118, 14288-14301.	2.6	5
67	Detection of Correlated Protein Backbone and Sideâ€Chain Angle Fluctuations. ChemBioChem, 2017, 18, 2016-2021.	2.6	5
68	Correlated motions of C′–N and Cα–Cβ pairs in protonated and per-deuterated GB3. Journal of Biomolecular NMR, 2018, 72, 39-54.	2.8	5
69	Interference between transverse cross-correlated relaxation and longitudinal relaxation affects apparent J-coupling and transverse cross-correlated relaxation. Chemical Physics Letters, 2006, 423, 123-125.	2.6	4
70	13C-detected HN(CA)C and HMCMC experiments using a single methyl-reprotonated sample for unambiguous methyl resonance assignment. Journal of Biomolecular NMR, 2006, 36, 259-266.	2.8	4
71	Solution NMR backbone assignment reveals interaction-free tumbling of human lineage-specific Olduvai protein domains. Biomolecular NMR Assignments, 2019, 13, 339-343.	0.8	4
72	Measuring 1H–1H and 1H–13C RDCs in methyl groups: example of pulse sequences with numerically optimized coherence transfer schemes. Journal of Magnetic Resonance, 2005, 172, 36-47.	2.1	3

#	Article	IF	CITATIONS
73	Full relaxation matrix analysis of apparent cross-correlated relaxation rates in four-spin systems. Journal of Magnetic Resonance, 2013, 226, 52-63.	2.1	3
74	Solution NMR backbone assignments of the N-terminal Zα-linker-Zβ segment from Homo sapiens ADAR1p150. Biomolecular NMR Assignments, 2021, 15, 273-279.	0.8	2
75	Enzyme Selectivity Fineâ€Tuned through Dynamic Control of a Loop. Angewandte Chemie, 2016, 128, 3148-3152.	2.0	1
76	Protein Allostery at Atomic Resolution. Angewandte Chemie, 2020, 132, 22316-22323.	2.0	1
77	Microbiotaâ€derived butyrate is an endogenous inhibitor of HIF prolylâ€hydroxylases. FASEB Journal, 2021, 35, .	0.5	0
78	On the use of residual dipolar couplings in multi-state structure calculation of two-domain proteins. Magnetic Resonance Letters, 2022, 2, 61-68.	1.3	0
79	Solution NMR backbone assignments of disordered Olduvai protein domain CON1 employing Hα-detected experiments. Biomolecular NMR Assignments, 2022, , 1.	0.8	0
80	Structural Investigation of a Putative Intrinsically Disordered Region Within Deleted in Colorectal Carcinoma That Regulates Protein Synthesis. FASEB Journal, 2022, 36, .	0.5	0
81	Butyrate Analogues Mimicking Hypoxia by the Chemical Stabilization of Hypoxia Inducible Factor (HIF). FASEB Journal, 2022, 36, .	0.5	0